Broadband EMFi-Based Transducers for Ultrasonic Air Applications

Joao L. Ealo, Fernando Seco, and Antonio R. Jimenez

***Abstract*—In this work, we explore the possibilities of electromechanical film (EMFi) as a new material for developing broadband transducers for ultrasonic air applications. The advantages of the EMFi film are its wide usable frequency range and easiness to use, making it highly suitable for self-made, customizable ultrasonic sensors. This paper presents theoretical and experimental information focused on the needs of the sensor's end-user, namely, frequency response, actual dynamic mass and Young's modulus, bandwidth, sensitivity, electromechanical dynamical model, acoustic response, and directivity. It is found empirically that the behavior of the film as an almost ideal piston-like acoustic source permits accurate prediction of the characteristics of transducers built on a developable surface. The results obtained represent the first step to more complex geometries, and, ultimately, to completely customizable field ultrasonic transducers.**

I. Introduction

Ultrasonic signals are widely used in robotic applications such as sound echolocation, identification of objects, local positioning systems, distance or proximity sensing, process inspection, quality control, etc. Among them, ranging is perhaps the most applied technique in robotics, due to its low cost implementation [1]. In general, most ultrasonic applications in air use the frequency range between 20 and 300 kHz. However, some of them require a maximum frequency not greater than 120 kHz in order to minimize the signal attenuation caused by absorbtion, e.g., robot navigation and localization at long ranges.

Nowadays, most robotic systems make use of either piezoceramic or capacitive transducers. The former are resonant devices with a high quality factor and correspondingly low bandwidth (typically less than 1/10 relative to their central frequency); they are very rugged and inexpensive. As a consequence of the applied damping method, they can achieve more bandwidth but their high sensitivity is reduced. In a general sense, the latter have a better performance than piezoelectric ones because they exhibit the highest bandwidth (about 30 kHz for some Polaroid models). Besides, they are the preferred choice when using coded signals [2], [3]. However, they are expensive and not very rugged.

Manuscript received August 17, 2007; accepted December 10, 2007.

The authors are with the Instituto de Automática Industrial, Consejo Superior de Investigaciones Cientificas, Arganda del Rey, Madrid, Spain (e-mail: jealo@iai.csic.es).

J. L. Ealo is also with the School of Mechanical Engineering, Universidad del Valle, Cali, Colombia.

Digital Object Identifier 10.1109/TUFFC.2008.727

Piezopolymers, most notably polyvinylidene fluoride (PVDF), have also been applied as ultrasonic transducers. Yet, their transmitting sensitivity is an order of magnitude lower than that of piezoceramics. PVDF film transducers are inexpensive, are more rugged than capacitive transducers, and have a bandwidth of about 8–10 kHz for a central frequency of 40 kHz. They are particularly attractive for air coupled applications because of their low impedance. Air ranging devices have been designed by Toda [4], [5] and Fiorillo [6]. However, their mechanical setup and principle of operation based on length variations make them not suitable when customizable acoustic fields applications are intended [7].

In particular, broad bandwidth is fundamental for applications that require signal modulation and codification in order to achieve multiple transducer operation (CDMA) and exploit the processing gain inherent to the signal structure. Nevertheless, most of the implemented systems are based on piezoelectric narrow-band ceramics for ranging measurements, which brings about three main difficulties: single-user access, lack of identification encoding, and ultrasonic noise sensitivity [8]. In view of this, there still remains a current demand to develop ultrasonic transducers that satisfy the trade-off among directivity, bandwidth, sensitivity, and cost. In this work, the use of the electromechanical film (EMFi) is put forward to fulfil this requirement.

A. The Electromechanical Film

Recently, cellular electret polymers have generated great interest due to their good storing charge capabilities and flexibility. The EMFi is among this new type of materials. Basically, this low-cost thin film is a microporous polypropylene foam with high resistivity and permanent charge after being polarized by the corona method. The resultant inner air voids act as dipoles which make it particularly sensitive to forces normal to its surface. When glued on a rigid substrate and excited by an external voltage, EMFi can be used as an actuator, operating always in thickness mode without influence of the substrate geometry [7]. The sensor mode of operation is the reciprocal to the actuator one. Its very low Young's modulus results in a very low acoustic impedance so that good adaptation to air is achieved. In view of this, EMFi has been used to build up acoustic transducers such as loudspeakers and microphones [9], physiological sensors [10], [11], keyboards, force position sensors [12], etc. The usable frequency range of the EMFi film for air applications begins at audible frequen-

cies and extends up to its measured resonance frequency (300 kHz). This makes it well suited to work as ultrasonic transducer in applications such as range measurements, local positioning systems [7], robot navigation, bat research [13], [14], ultrasonic imaging [15], [16], etc. In addition to this, the EMFi film can be easily stuck to non-flat substrates, which paves the way for the design of ultrasonic transducers with customizable radiating patterns.

This paper reports the results of our research with the EMFi film with the purpose of building broadband, highly customizable field ultrasonic transducers for air applications. Valuable end-user information with regard to the transducer design process is presented by means of experimentation results and theoretical analysis. Namely, the following aspects of the EMFi as an ultrasonic transducer were treated:

- Considerations on mechanical fixation of the film to the substrate;
- Vibration mode characterization and quantification of the effects on the "ideal" response caused by frequency changes and curvature of the substrate;
- Frequency response characterization;
- Modelling and validation of the electromechanical response which permits predicting the effects of mechanical loading, sample stacking, etc.;
- Theoretical computation of the acoustic field for different substrate transducers and matching to experimental results.

II. Materials and Methods

A. Transducer Prototype Fabrication

The EMFi film used in this work has been provided by Emfit Ltd. (Vaajakoski, Finland). It is detailed as Emfit Film, product number HS-03-20BR AL1, metallized on one side only and without a pre-aging process. The product itself has the appearance and flexibility of a paper sheet.

The transducer's active part is manually tailor-made by die cutting the foil to a specific shape and size with a scissor or an edge cutter. Following this, the film is fixed with an adhesive to a solid substrate shaped to the desired transducer geometry; this is easily done given the flexibility of the EMFi film. Therefore, sticking EMFi on substrates of complicated curved geometries is always possible whenever the substrate surface is either a solid of revolution whose generatrix consists of straight lines, or a polyhedron. Alternatively, the EMFi film can be first fixed on a flat flexible sheet, which is then bent to conform to the required shape. We experimented with both methods of fabrication of cylindrical transducer prototypes and found no differences in the vibratory response of the transducer, within our experimental error margin, and for radii of curvature larger than 5 mm. It's possible that more curved substrates will induce a stress on the EMFi film and modify its behavior, and that is a point for future research.

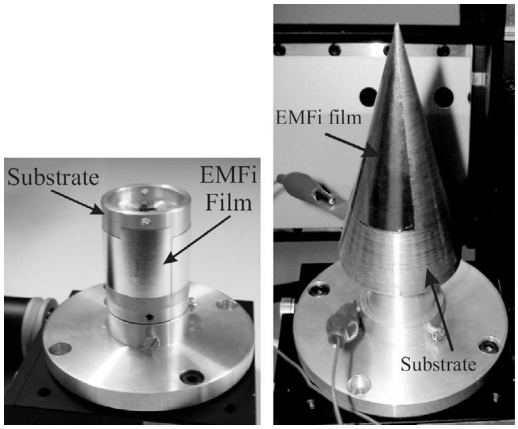

Fig. 1. Fabricated transducers using conical and cylindrical aluminum substrates and plastic tape as adhesive.

As a consequence, we choose the first fabrication method described because it is easier and more reliable.

B. Substrate Geometries

In this work, three different geometries of solid aluminum substrates were analyzed, i.e., flat, cylindrical, and conical. Several 20-mm flat-square transducer prototypes were fabricated in order to model the dynamical mechanical response of the transducer by means of interferometric measurements on a grid of 361 evenly spaced points on the emitter surface. As an intermediate step to more complicated curved geometries such as spheres, ellipsoids, etc., cylindrical transducer prototypes of 30-mm diameter and 20-mm height were fabricated and tested. Besides, a 180° cylindrical transducer was specially fabricated with the aim of validating the developed acoustic model. Finally, instead of using several cylinders of different diameters, a conical aluminum substrate was specifically used in order to state, from interferometric measurements throughout the surface, the effect of the substrate curvature on the mechanical response. Fig. 1 shows EMFi-based transducer prototypes built on cylindrical and conical substrates.

C. Fixation of the Film

Basically two adhesive types were used in the fabrication process of the transducer prototypes. First, an electrically conductive epoxy paste (ECP) was utilized for gluing the film to the substrate. Second, a XYZ-axis electrically conductive plastic tape (ECPT) was employed in order to obtain a more homogeneous support of the film. In addition to this, a common nonelectrically conductive double-sided tape (NCPT) was also evaluated. Experimentation was also conducted in order to measure the performance of the emitters when no adhesives were employed, i.e., the active material was just clamped on a flat substrate.

D. Experimental Setup

Fig. 2 illustrates a block diagram of the experimentation equipment used in this work. This instrumentation

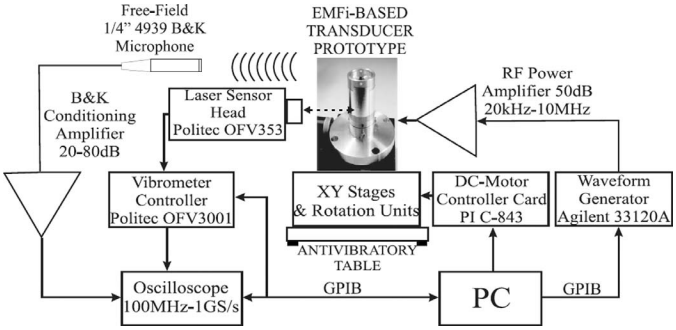

Fig. 2. Experimental setup.

consists of four main parts, i.e., the transducer excitation equipment, the acoustic pressure measurement channel, the laser-based Doppler vibrometer, and the servo-controlled motion units. The EMFi-based transducers were located on the servo-controlled motion units, which allow arbitrary displacements and rotations of the samples, in order to measure the velocity profile throughout the surface as well as the resultant acoustic radiating pattern. Interferometric measurements of the velocity surface of the transducer prototypes were carried out using a laser Doppler vibrometer from Polytec GmbH (Waldbronn, Germany). Sensitivities of 5 mm/s/V and 25 mm/s/V were used for measurement in the frequency range between 30 and 400 kHz. Special care was taken so as to avoid misalignment with the laser beam. We always checked to ensure that the substrates were free of vibrations. Air-borne acoustic measurements were accomplished by locating, at a distance of 30 cm far on the principal axis, a free-field calibrated condenser microphone from Brüel & Kjær (1/4″-4939; Nærum, Denmark). The protection grid was removed in order to get maximum sensitivity up to 100 kHz. With regard to the excitation equipment, short tone-burst sinusoidal signals were used to avoid the creation of a standing wave field. Wideband linear chirp excitation was also used in order to obtain the mechanical frequency response of the prototypes in the frequency range of 30–400 kHz.

Complex electrical impedance measurements of the fabricated prototypes were also taken to corroborate the frequency response of the samples.

III. Modelling of the EMFi Actuator Response

The modelling theory of electrostatic transducer has been widely reported in the literature [17], [18]. In regard to the EMFi film, static models of the electromechanical properties have already been reported by [19] and [20]. Also, a 3D finite element static model in which the EMFi is considered as made of polarized lens-like cavities is presented in [14]. In that work, as the film was microscopically modelled, the physical relationship between the resonant frequency and the cavity shape was demonstrated. Besides, the effect of the charge density on the displacement amplitude is shown. Despite the fact that a better understanding of the physical behavior of the EMFi film

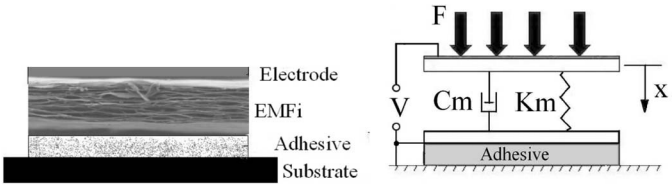

Fig. 3. EMFi-based transducer and its 2nd order mechanical model.

is provided, not enough end-user practical considerations, based on experimentation, are given with regard to the equivalent dynamic mass of the film, the dynamic Young's modulus, the transient response, the curvature effect, the resonant frequency tuning, etc. In view of this, a second-order dynamic mechanical model of the EMFi film was developed and identified in this paper. This model is intended to be used as a tool for optimizing the electronics design and predicting the response in the air, under different types of excitation, mass addition on the transducer surface, and stacking.

With respect to the acoustical field created by the vibratory response, a computational model was also required. As one of the observed advantages of using EMFi film as active material for fabricating ultrasonic transducers is that it can be adhered to substrates with curved geometries without significant changes in the thickness mode of vibration, the development of computational acoustic models proves to be crucial in the fast customization of the transducer's resultant farfield emitting pattern. Hence, in this work, as a first step to more complicated geometries and numerical methods of solution, an analytical acoustic model of a finite emitter that conforms to cylindrical symmetry has been revised and validated. The electromechanical acoustical modelling of the EMFi film response is briefly presented below, as well as the model validation results.

A. Dynamic Electromechanical Model

The electromechanical model of the EMFi film describes the change in the film thickness when an ac external voltage is applied to the transducer's electrodes. Fig. 3 shows a cross section of a transducer prototype. As observed, the EMFi film itself, in the middle, resembles an accordion because it consists of a central foam layer surrounded by two 10-μm-thick solid polypropylene skin layers. The upper layer of vaporized aluminum and the adhesive act as electrodes. Considering this, the general response of the EMFi-based actuator was modelled as shown in Fig. 3. The lumped parameter linear model estimates the active material displacement, represented by x, due to the applied force distribution F. In Fig. 3,

- m is the effective dynamic mass of the transducer. It is considered as the sum of the upper electrode mass and a fraction of the EMFi material mass.
- K_m is the combined dynamic stiffness due to the EMFi's air voids and its solid part.

C_m is the damping coefficient which encloses the viscous losses in the internal EMFi material structure and the mechanical impedance of the air.

V is the driving voltage applied to the transducer.

x_0 is the thickness of the polarized EMFi material at equilibrium, as provided by the manufacturer. A typical value of $\sim$70 μm is given.

As the EMFi is permanently polarized, it is initially preloaded by a force F_0, which is given by $F_0 = K_m\delta = \frac{q_0^2}{2\varepsilon A}$, where q_0, ε, and A are the stored charge at equilibrium, the electric permittivity, and the transducer area, respectively, and δ is the respective initial thickness variation because of the electrostatic attraction force. At equilibrium, no spring response from either the adhesive or the EMFi film is considered. In addition to this, the resultant dynamic system model was obtained under the assumption that the vibration takes place around x_0. The capacitance of the EMFi film is considered to vary according to $\frac{\varepsilon A}{x_0 - x}$. Using the charge formulation and the generalized coordinates x and q, the Lagrange's equations read:

$$m\ddot{x} + C_m\dot{x} + K_m x - \frac{(q_0+q)^2}{2\varepsilon A} = F, \tag{1}$$

$$\frac{x_0 - x}{\varepsilon A}(q_0 + q) = V. \tag{2}$$

In the equations, note the quadratic relationship between the force and voltage. Besides, it is also shown that the motion of the mass tends to complicate this relationship. Assuming that $q \ll q_0$, $x \ll x_0$ and that the driving voltage may be divided into a large bias voltage V_{dc} and a small signal voltage V_{ac}, and that the external force F is null in actuator mode of operation, it is possible to linearize (1) and (2) so that

$$m\ddot{x} + C_m\dot{x} + K_m x = \frac{q_0}{x_0}V_{ac}. \tag{3}$$

This resultant equation approximates the dynamical response due to an external ac excitation voltage. It must be pointed out that the loading of the voltage source by the transducer has not been taken into account. Eq. (3) can be converted to frequency form by means of the Laplace transform, as given in (4):

$$\frac{\dot{x}}{V} = \frac{\frac{q_0}{x_0 m}\frac{\omega}{\omega_n}}{\sqrt{(1 - \left(\frac{\omega}{\omega_n}\right)^2)^2 + \left(2\zeta\frac{\omega}{\omega_n}\right)^2}}. \tag{4}$$

B. Farfield Radiation from a Finite Cylindrical Source

As a first step to develop a transducer with more complicated geometries, in this work, the behavior of cylindrical substrate EMFi-based emitters was studied and measured. In view of this, the theoretical background of finite cylindrical sources is briefly presented below [21], [22].

The pressure field in cylindrical coordinates of a source that conforms to cylindrical symmetry, obtained as the general solution of the wave equation, is given by

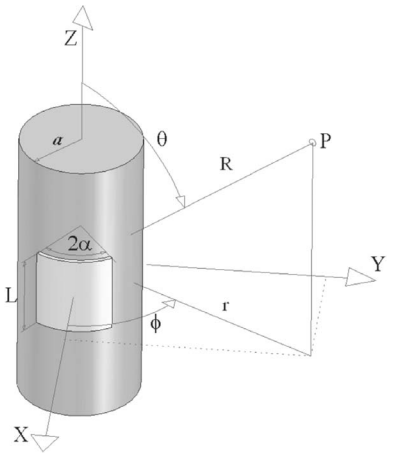

Fig. 4. Transducer on a cylindrical substrate and conventions.

$$p(r,\phi,z) = i\rho ck\mathcal{F}_\phi^{-1}\mathcal{F}_z^{-1}[\dot{W}_n(a,k_z)\frac{H_n(k_r r)}{k_r H_n'(k_r a)}], \tag{5}$$

$$\dot{W}_n(a,k_z) = \mathcal{F}_\phi\mathcal{F}_z[v_n(a,\phi,z)], \tag{6}$$

where a, ρc, k, r, H_n, and $\dot{W}_n$ represent, respectively, the radius of the cylinder, the characteristic impedance of the propagation medium, the wavenumber, the azimuthal far-field distance measured from the origin, the first-kind Hankel's function of n^{th} order, and the two-dimensional Fourier transform of the transducer surface velocity profile. The terms k_z and k_r are separation constants related to the wavenumber in the equation $k_r = \sqrt{k^2 - k_z^2}$. In (6), v_n is the normal component of the velocity of the vibrator cylindrical surface. See Fig. 4 for conventions. Following a relation similar in concept to Rayleigh's first integral formula, it is possible to write (5) as

$$p(r,\phi,z) = i\rho ck\sum_{n=-\infty}^{\infty}(-i)^n e^{in\phi}\frac{1}{2\pi}\times \int_{-\infty}^{\infty}\dot{W}n(a,k_z)\frac{H_n(k_r r)}{k_r H_n'(k_r a)}e^{ik_z z}dk_z. \tag{7}$$

As the source is finite, it is not possible to analytically integrate over k_z in the previous equation. In view of this, an asymptotic method called the stationary phase approximation is applied to calculate the integral when r is very large compared to the dimensions of the transducer. In addition to this, the Hankel function is replaced with its far-field formula. Applying the stationary phase method for a constant velocity profile, the far-field radiating pattern in spherical coordinates can be approximated as

$$p(R,\theta,\phi) \approx \frac{\rho_o c}{2\pi^2}\frac{e^{ikR}}{R}\sum_{n=-N}^{N}(-i)^n e^{in\phi}\frac{4v_n\alpha L\mathrm{sinc}(n\alpha)\mathrm{sinc}(kL\cos\theta)}{\sin\theta H_n'(ka\sin\theta)}, \tag{8}$$

where N is the closest integer to $ka\sin\theta$, $2L$ is the length of a piston of radius a and angular width 2α, and the center

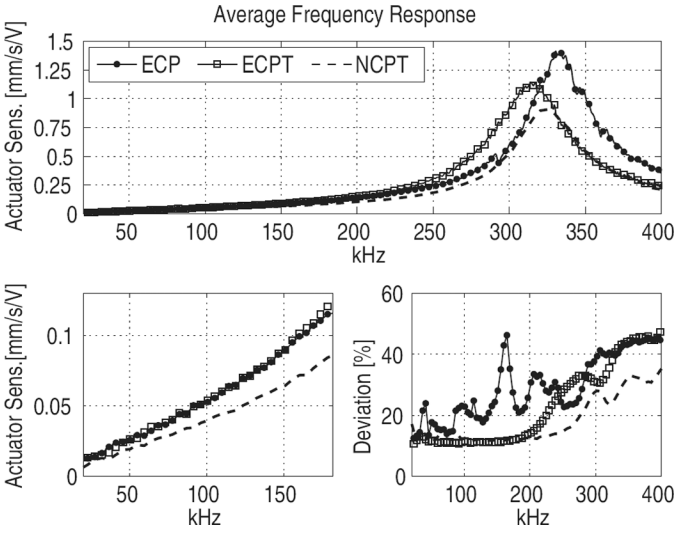

Fig. 5. Average frequency response of emitters fabricated with three different adhesive types, obtained from 361 different measurement points on each transducer. Standard deviation as a percentage of the average response.

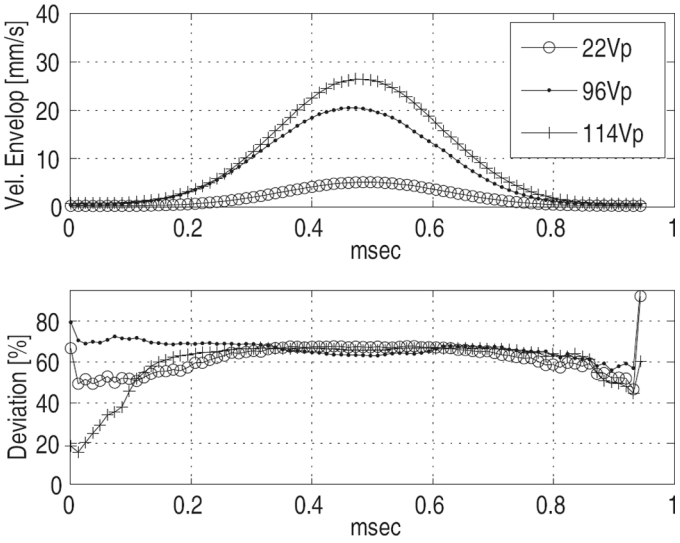

Fig. 6. Average velocity on flat emitter surface at resonance (320 kHz) for three different excitation levels. Obtained from the average envelop of the responses of 361 different measurement points to a 1-ms Gaussian-windowed tone signal. Standard deviation as a percentage of the average response.

of the vibrating surface is at $\phi = 0$. The normal velocity is zero everywhere except on the patch. As the baffle is considered infinite in length, it is possible to obtain an analytical solution that allows estimation of the far-field acoustical response. In the frequency range of interest, for which $8 < ka < 30$, no further approximations of (7) are used.

IV. Results

A. Transducer Frequency Response

First, the influence of the adhesive used to fix the film to the substrate on the frequency response of the transducer was explored. The surface motion of the 20 mm by 20 mm flat transducer prototypes was measured on 361 equally spaced different points arranged into a 19 by 19 grid of 1-mm side unit squares. This procedure was accomplished for prototypes fabricated using ECP, ECPT, and NCPT. Fig. 5 shows the average frequency response of the three different prototypes when a 30–400 kHz chirp excitation signal is applied. The percentage deviation of the response is also illustrated. It is clearly appreciated that the measured points exhibit a second-order behavior with resonant frequency around 320 kHz. In the low frequency range (30–100 kHz), approximate average actuator sensitivities of 63 pm/V (picometer per volt), 95 pm/V, and 98 pm/V were calculated when NCPT, ECPT, and ECP, respectively, were used. As expected, the measured electrical impedance of the ECPT was significantly lower than that of the NCPT. For this reason, the only significant difference between their respective frequency responses is a gain factor of about 30% (see Fig. 5). Meanwhile, the frequency response results were almost identical when either ECPT or ECP was used below 200 kHz.

A significantly lower variability of the frequency response of the measured points was obtained when the plastic adhesive tapes are used. On the other hand, the most irregular frequency response throughout the whole frequency range was obtained with ECP. This can be attributed to an inappropriate manual application of the epoxy paste along with an irregular cross/through conductivity of the deposited layer. Apart from a more irregular support when using ECP, no effect of the type of adhesive on the average transducer response was observed in the frequency range of interest. This can be explained by the fairly larger elastic modulus of the adhesives in comparison with the EMFi's stiffness.

Using tone burst signals, it was observed that the percentage deviation of the average response remains unchanged as the amplitude of the excitation is increased up to 114 Vp. This indicates that the variability of the frequency response is not directly related to the amplitude of the motion but to the frequency of the vibration (see Fig. 6). Besides, the EMFi film conforms to linearity with respect to increasing voltage when excited with amplitudes below 120 Vp. No experimentation at higher voltages was conducted because of the RF power amplifier maximum voltage limitation. However, according to [13], excitation voltages up to 300 Vp are allowed without risk of electrical breakdown.

To this end, the best results, in terms of actuator sensitivity, variability of the response and easiness of fabrication, are obtained using the same adhesive, i.e., ECPT. Fig. 7 shows the frequency response of four different 20 mm by 20 mm flat emitters fabricated using ECPT. From this, it can be stated that frequency response of the EMFi transducers may become irregular after 150 kHz. The resonant frequency appears within the range of 280 to 330 kHz.

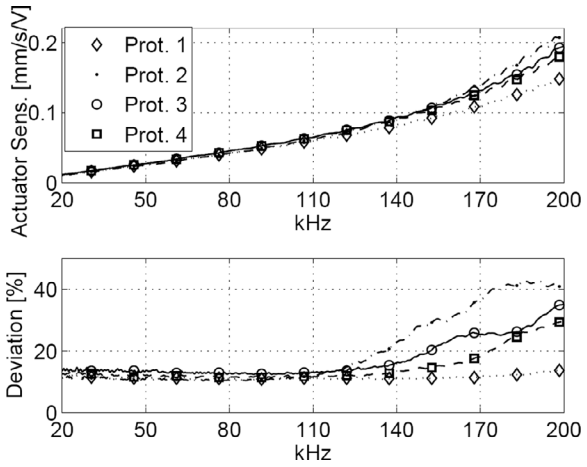

Fig. 7. Average frequency response of four different flat square transducer prototypes fabricated using ECPT. Obtained from interferometric measurements of 361 different points on the surface. Standard deviation as a percentage of the average response.

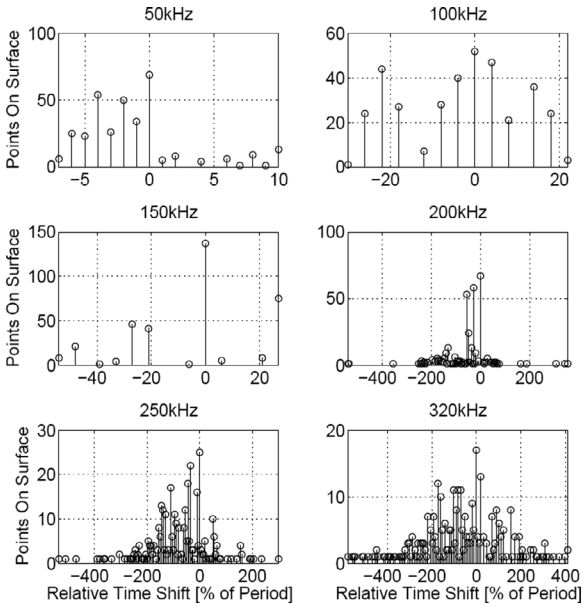

Fig. 8. Analysis of the piston-like behavior of the flat transducer surface. The figure shows the distribution of the relative phase shift of 361 measured points on the transducer's surface, determined by correlation. As observed, the mean phase shift increases with frequency, particularly above 100 kHz.

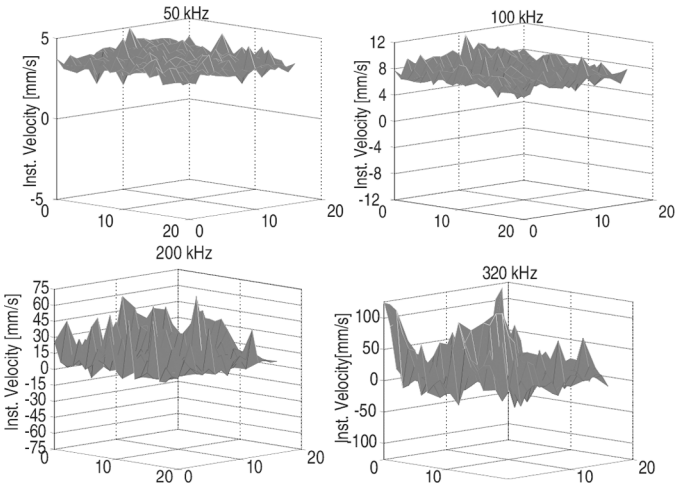

Fig. 9. Instantaneous spatial distribution of the velocity over a flat transducer surface at different frequencies.

However, the response within the range of interest, below 150 kHz, is almost the same for all prototypes.

High repeatability was found between different samples, which indicates that the assembling procedure is not critical, even when done by hand.

When no adhesive was used, the edges of the square film patch were clamped with a flat thin plate mechanically fixed to the substrate; no tension was applied to the film. Despite the flatness of the substrate being guaranteed, it was not straightforward to achieve a homogeneous contact between the EMFi film and the substrate. As a consequence, an erratic and irregular dynamic response of the surface was measured. As a matter of fact, the best results are obtained when double-sided plastic films were used, i.e., NCPT and ECPT. In principle, clamping the electromechanical film is not recommended when covering substrates with non-flat or curved geometries because it makes the transducer design process and the acoustic field customization much more complicated.

B. Piston-Like Vibration Mode

The instantaneous vibratory response of the whole flat transducer surface was analyzed in order to state the characteristic vibration mode.

To quantify the "in-phase" motion of the flat EMFi-based transducers, a correlation analysis between the time excitation voltage and the respective time velocity response of the measurement points was carried out. Gaussian-windowed tone signals were used in order to measure the instantaneous phase difference distribution as the frequency increases. Fig. 8 depicts histograms of the relative phase shift of the velocity of a given point on the transducer surface with respect to the mode at different frequencies. It can be concluded that, below 100 kHz, the phase differences in the velocity profile of the surface are not greater than 20% of the period. This characteristic, in addition to the low variability of less than 18% (see Fig. 7) in the same frequency range, enables us to state that the EMFi emitters behave piston-like. Beyond 100 kHz, the velocity profile becomes uneven. However, the observed fluctuations of the instantaneous time velocity profile and of the corresponding generated acoustic field do not match with the shape of the known higher-order vibration modes of a plate, so we assume that they are caused by random nonuniformities of the electromechanical properties of the EMFi film (see Fig. 9). Hence, in the frequency range of interest, the acoustic field generated conforms to the theoretical radiating pattern of an ideal square piston, as it is depicted in Fig. 10. Simulations with the piston model suggest that the variations in the velocity profile are smoothed over by the integration process of the acoustic field. As

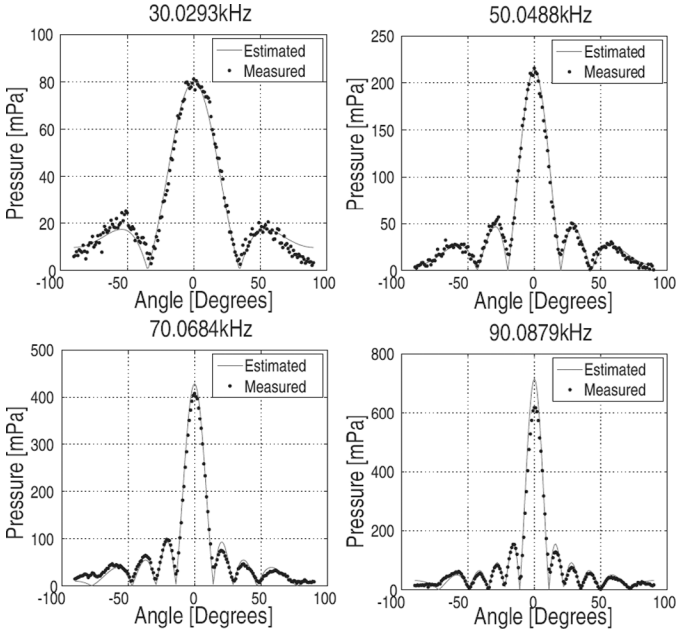

Fig. 10. Horizontal farfield radiating directivity pattern of a flat 20 mm by 20 mm EMFi-based emitter in the frequency ranges of interest. Model vs. measurements.

the frequency increases, there is a disagreement between the simulated and the experimental results of up to 30% for some transducers, which may be due to the effect of the random velocity distribution, in combination with the acoustic frequency absorbtion, not considered in the estimation.

Yet, the almost ideal piston response is not guaranteed at higher frequencies as the effect of the phase differences and larger variability of the velocity profile may become significant. Current research is being conducted in order to state the limit frequency of the piston-like behavior of the EMFi-based emitters and its impact on the acoustic field.

C. Effect of Substrate Curvature

In order to quantify the effect of conforming the EMFi film to cylindrical substrates of different radii of curvature on the dynamical response, the fabricated conical prototype was used. Interferometric longitudinal measurements throughout the active surface were accomplished. In Fig. 11, the frequency response magnitude does not significantly change as the radius of curvature diminishes, showing similar values to those obtained with a flat substrate. The small variations of the slope of the frequency response fall well within our experimental standard deviation margin. This unchanged behavior is because the nominal size of the inner voids of the EMFi film is several orders of magnitude smaller than the minimum radius of curvature in the cone. The air voids have lateral dimensions of 10 μ to 100 μm and vertical dimensions of 3 μm. Small radii of curvature are therefore possible in transducer design as long as good adhesion is guaranteed. Besides, the inherent flexibility of the cellular structure of the film makes it possible to

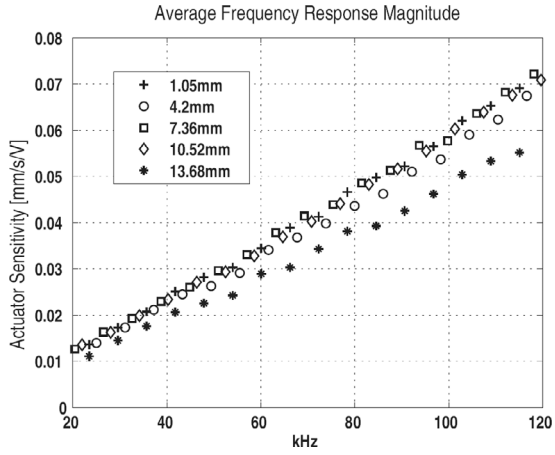

Fig. 11. Frequency response of the fabricated conical substrate emitter at different radius of curvature.

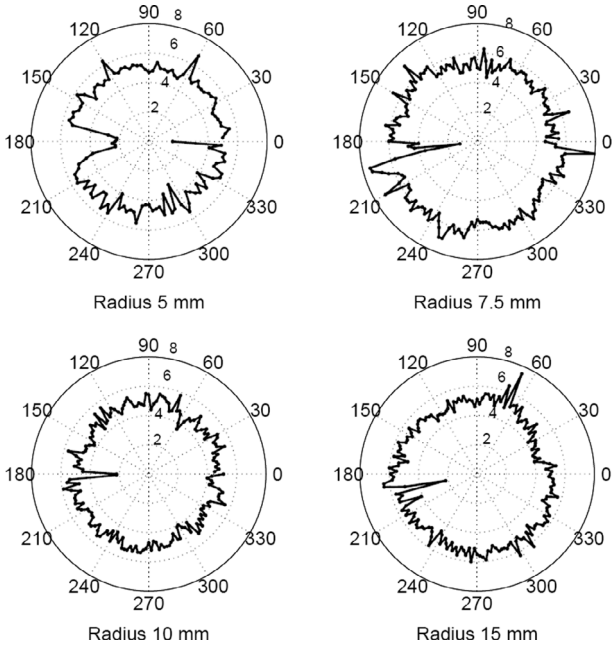

Fig. 12. Instantaneous velocity profile of four cylindrical emitters with different radius of curvature. Measurements at 70 kHz and maximum velocity amplitude. Velocity amplitude in mm/s.

wrap it around cylindrical and conical substrates without creating creases or inducing important normal stresses.

Fig. 12 shows the instantaneous velocity profile of four cylindrical prototypes of different radius under the same excitation signal. The measurements were obtained at maximum velocity amplitude during a harmonic cycle. It is easily noticeable that some points on the circumference either remain static or show a velocity higher than the average. Most important, the vibratory response of the four prototypes compares well to the ideal breathing mode. Besides, the velocity amplitude remains the same in the four plots, which corroborates the results obtained with the conical substrate.

As a conclusion, and as far as our experimental results go, single foil EMFi transducers behave in the thickness

TABLE I
OPTIMIZATION RESULTS OF THE 2ND-ORDER MODEL FITTING FOR A FLAT EMFI TRANSDUCER AND THREE DIFFERENT ADHESIVES.

Adhesive	$\frac{q_0}{x0m}$	ζ	ω_r (kHz)
ECP	3.196×10^5	0.057	332.72
ECPT	2.835×10^5	0.064	312.38
NCPT	2.196×10^5	0.059	323.88

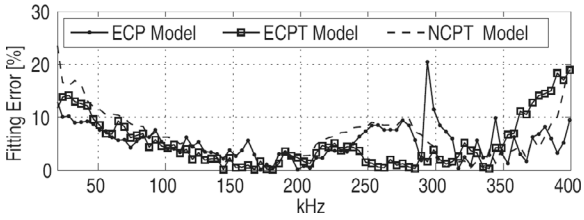

Fig. 13. Optimization results. Estimation error.

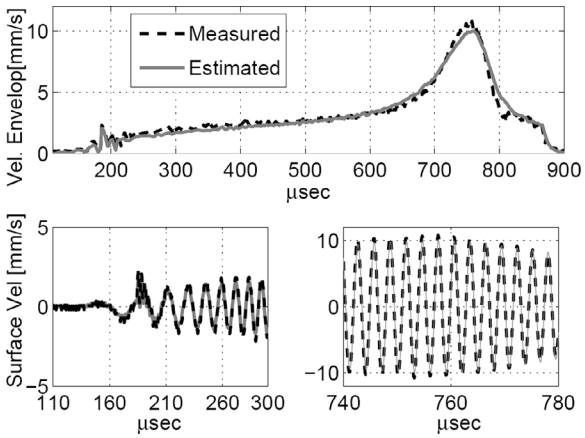

Fig. 14. Broadband time velocity responses obtained from model and experimentation with a transducer fabricated with ECPT. Linear chirp excitation from 20 kHz to 400 kHz was used.

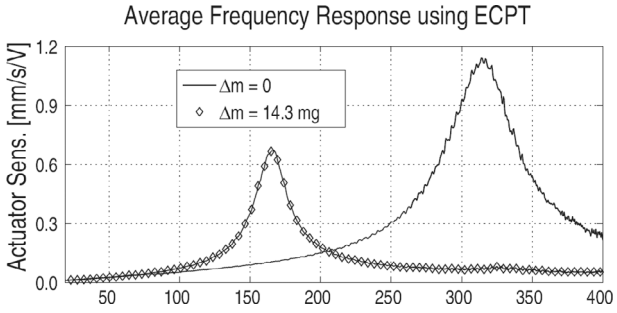

Fig. 15. Frequency response of a flat emitter prototype after adding a load mass, Δm, on the upper electrode.

mode of vibration, and are not influenced by the curvature of the substrate, at least down to 1 mm. This capability of the EMFi material makes it suitable to easily combine different geometries in order to fabricate ultrasonic emitters with an arbitrary customizable field.

D. Electromechanical Model Identification and Validation

The unknown parameters of the EMFi's 2nd-order model of Section III-A are found by fitting the gain from the experimental frequency response to the model (4). The tuned model parameters were $\frac{q_0}{x_0 m}$, ζ and ω_n. The variables ζ and ω_n represent the damping ratio and the natural frequency, respectively, and are related to each other in the equation $\omega_r = \sqrt{1-\zeta^2}\omega_n$, where $\omega_n = \sqrt{\frac{K_m}{m}}$, and ω_r is the resonant frequency. We considered three different sets of parameters, depending on the adhesive used (ECP, ECPT, and NCPT).

Table I summarizes the results obtained for the three unknown parameters. In the frequency domain, a residual error not greater than 15% between the real data and the estimated transfer function was obtained in the 30–350 kHz frequency range (see Fig. 13). The temporal response of the transducer to chirp waveforms covering the frequency range of interest was estimated perfectly with the model, as depicted in Fig. 14.

In order to determine the effective dynamic mass of the EMFi-based transducers from the tuned parameters, a small mass of adhesive tape of approximately $\Delta m = 14.3$ mg was stuck on the upper electrode of an ECPT flat prototype. As a consequence, the resonant frequency was shifted to 165 kHz (see Fig. 15). Using the relationship expressed in (9), it is possible to state the effective dynamic mass m of the transducer:

$$\frac{m+\Delta m}{m} = \left(\frac{[\omega_n]_m}{[\omega_n]_{m+\Delta m}}\right)^2. \tag{9}$$

From this, $m \approx 5.49$ mg, which is about the 40% of the total mass of the EMFi film used in the emitter fabrication, calculated from the density and thickness given by the manufacturer. Consequently, the corresponding dynamic elastic modulus E is 3.715 MPa, according to $K_m = \frac{EA}{x_0}$. This value does not well agree with that of the manufacturer ($0.5 \pm 25\%$ MPa) or those given in [16] (2 MPa) and [19] (0.89 MPa). We believe that this is caused because the reported magnitudes were either estimated under quasi-static experimentation or based on a nonexperimental assumption of the dynamic mass of the transducers.

As the measured resonant frequency of the fabricated transducers may vary from 290 to 320 kHz, with no significant changes in the damping ratio, it can be established as a rule of thumb that the dynamic mass of the transducer is $40 \pm 5\%$ of the total calculated EMFi mass of the transducer. The low values of ζ indicate a quite good matching with the air, as the response is underdamped.

An EMFi's quality factor of 8.3 was also estimated which compares to the PVDF's one (4–6) reported by [4] for cylindrical PVDF airborne ultrasonic transducers. From the dynamical modelling, the approximated bandwidth of the EMFi film can be estimated as

$$\mathrm{BW} = 2\zeta\omega_{\mathrm{nom}}\sqrt{\frac{0.4\rho_{\mathrm{EMFi}}}{0.4\rho_{\mathrm{EMFi}} + \rho_{\Delta m}}}, \tag{10}$$

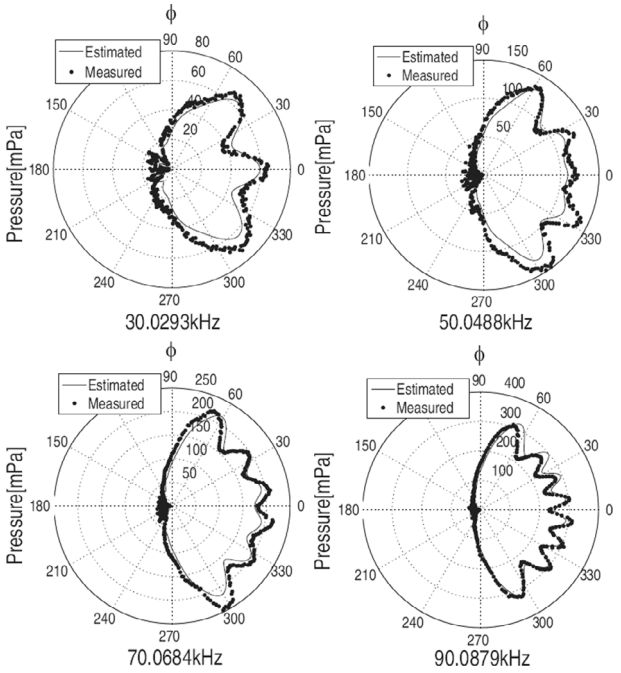

Fig. 16. Comparison of model and experimental results for the horizontal farfield radiating directivity pattern of a 180° cylindrical transducer with aspect ratio $\frac{L}{2a} = \frac{2}{3}$. ($L = 20$ mm, $\alpha = 90°$, $a = 15$ mm). Model vs. measurements.

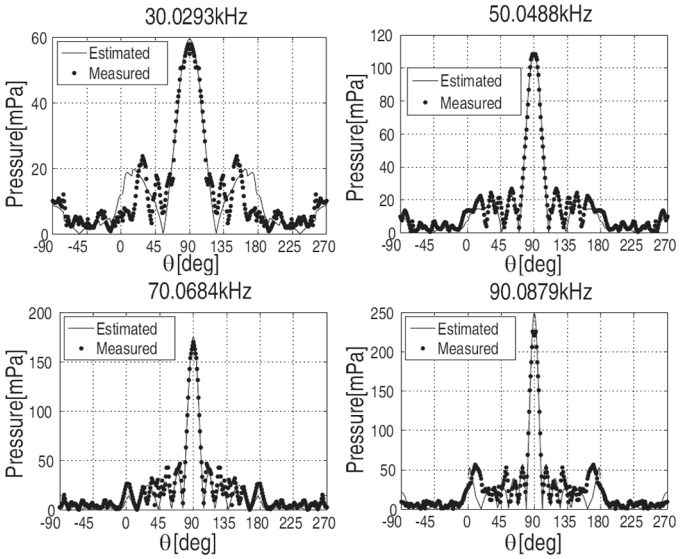

Fig. 17. Comparison of model and experimental results for the vertical farfield radiating pattern directivity of a 180° cylindrical transducer with aspect ratio $\frac{L}{2a} = \frac{2}{3}$. ($L = 20$ mm, $\alpha = 90°$, $a = 15$ mm).

where ρ_{EMFi} and $\rho_{\Delta m}$ are the densities per unit area of the EMFi film (0.034 3 kg/m^2) and of the tape used to shift the resonant frequency (0.035 7 kg/m^2 in this work), respectively, and ω_{nom} is the chosen nominal resonant frequency of the EMFi film in air, i.e., 315 kHz. Eq. (10) results are valuable for the end-users interested in narrowband applications around resonance. However, it must be emphasized that the film has a usable frequency range that begins at audible frequencies and extends up to 300 kHz, which makes it suitable when spread spectrum techniques are required.

E. Acoustic Measurements and Model Validation

As stated earlier from velocity and pressure measurements, an almost ideal piston dynamic behavior was measured below 100 kHz regardless of the radius of curvature of the substrate. Consequently, the acoustic piston response was measured in the frequency range of 30–100 kHz. Figs. 16 and 17 show the estimated and measured emitting patterns of the 180° cylindrical substrate EMFi-based emitter fabricated using EMFi film and ECPT as adhesive at four different frequencies. In the figures, the principal axis corresponds to 0 and 90 degrees in the horizontal and vertical patterns, respectively, at 30 cm far from the source.

With regard to the azimuthal pattern, the maximum estimation error was not greater than 18%, which represents less than 3 dB in the sound pressure level. The previously measured variability of the velocity throughout the transducer surface below 100 kHz did not have a significant effect on the corresponding acoustic field, which, for all purposes, resembles the ideal piston acoustic response (see Fig. 16). It is also observable that the acoustic model properly predicts the experimental interference pattern of the transducer, even for the backscattered field. Similar estimation errors in the vertical pattern were obtained. It is important to point out that the assumption of an infinite baffle boundary condition in the model restricts the validity of the model to approximately 34° in the vertical angle, because the aspect ratio of the measured transducer is $\frac{L}{2a} = \frac{2}{3}$. Despite this, as the radiating pattern becomes very directive, the developed model was able to estimate even the first sidelobes of the far-field pattern (see Fig. 17). As the frequency increases, the error estimation at 100 kHz may grow to 30% for some transducers. This might be caused by medium losses, microphone orientation errors, irregular sensitivity of the microphone around 100 kHz, or cancellation effects coming from the nonhomogeneity of the vibrating mode, among others.

From acoustic measurements, sound pressure level (SPL) values ranging from 66 to 79 dB can be obtained using omnidirectional cylindrical transducers (20 mm high and 30 mm in diameter at 30 kHz and 100 kHz, respectively) and a driving voltage of 100 Vp at 30 cm on principal axis. From developed models, this SPL range can be augmented up to 81 to 91 dB with an excitation voltage of 300 Vp without risk of electrical breakdown. With regard to the 20-mm flat-square transducers, typical SPL values range from 70 to 87 dB for frequencies between 30 and 100 kHz (see Fig. 10). This acoustic output can be modified by stacking foils, resizing the EMFi-based transducer, or improving the piezoelectric activity of the cellular polymer (see [23]). On the other hand, for narrow-band applications, it is also possible to shift the frequency response by properly adding mass to the upper electrode.

V. Discussion and Conclusions

In this section, we summarize the main findings of our research so far, with special emphasis on transducer fabrication issues for end-users of the EMFi material.

With regard to the manual fabrication process using plastic tapes, it is important to avoid the creation of creases in the process of fixing the film or the adhesive to the substrate. There are no significant differences in the film behavior when using either a scissor or an edge cutter to obtain the desired shape. Best results were obtained with ECPT as adhesive. In general, using the ECPT has proved to be easy, fast, and reliable. In addition to this, the electrical losses are minimized and a homogeneous support of the EMFi film is guaranteed.

The motion of the upper electrode of the film is not affected by the substrate curvature, at least down to a radius of curvature of 1 mm. Its observed thickness mode operation characteristics do not significantly vary, provided that special care is taken in the transducer fabrication process. A good surface finishing and the homogeneity of the adhesion, in combination with an even application, prove decisive in order to obtain repetitive results.

Despite the nonhomogeneous charge distribution throughout the electret and the irregular layout and size of the permanently polarized air voids inside the material, the measured dynamic mechanical/acoustical response fairly emulates the behavior of a piston throughout the whole frequency range of interest. No plate vibration modes were observed. The points on the edges of the transducers showed no higher deviation than those of the rest of the surface, i.e., no border effects were observed.

Nevertheless, from the analysis of the interferometric measurements, random vibration patterns of the EMFi film have been observed over 150 kHz. Considering that the size of the air cavities inside the EMFi film is not uniform and its layout is irregular, saturation in the motion might take place at some particular points on the surface as the amplitude of the motion increases. This behavior, along with the irregular sensitivity distribution throughout the active surface, explains the observed degradation of the breathing mode of vibration, where phase differences in the velocity profile become considerable.

The EMFi's capability of vibrating as a piston without the influence of the substrate geometry offers the possibility of customizing the shape of the far-field acoustic pattern and its magnitude, with advantages over other customizable transducer materials, e.g., PVDF. Provided that the substrate surface is developable, either analytical or numerical models of the acoustic field can be implemented in order to optimize the transducer design process. So far, hemispherical and 2D omnidirectional polar acoustic fields have been easily achieved and measured at frequencies below 100 kHz. Currently, research is being conducted in order to achieve 3D broadband omnidirectional emitting patterns using the EMFi film.

The observed variation of the frequency of resonance is due to differences in the properties from sample to sample. The frequency response variability in the range of interest remains below 15–20% and the actuator sensitivity can be approximated to 95 pm/V regardless of the substrate curvature. It must be pointed out that, although the EMFi transducer can be operated at its resonant frequency with the highest sensitivity, in this paper we have been more concerned with characterizing the material in the frequency range below resonance, which is more suitable for ultrasonic air systems that require broader frequency response.

The constant velocity profile, not influenced by the curved substrate geometry, the sound pressure level obtained in the 30–100 kHz frequency range, and the ease of use with ECPT as adhesive make the EMFi actuators well suited for applications where low cost, wide/narrow bandwidth, good coverage area by customization of the acoustic far field, and low infrastructure are required, i.e., ranging, robot navigation, positioning systems, etc.

References

[1] G. G. Yaralioglu, A. S. Ergun, Y. Huang, and B. Khuri-Yakub, "Capacitive micromachined ultrasonic transducers for robotic sensing applications," in *Proc. IEEE/RSJ Int. Conf. Intell. Robots Syst.*, 2003, pp. 2347–2352.

[2] H. Peremans, K. Audenaert, and J. V. Campenhout, "A high-resolution sensor based on tri-aural perception," *IEEE Trans. Robot. Automat.*, vol. 9, no. 1, pp. 36–48, 1993.

[3] J. Ureña, M. Mazo, J. J. García, A. Hernández, and E. Bueno, "Classification of reflectors with an ultrasonic sensor for mobile robot applications," *Robot. Autonom. Syst.*, vol. 29, pp. 269–279, 1999.

[4] M. Toda, "Cylindrical PVDF film transmitters and receivers for air ultrasound," *IEEE Trans. Ultrason., Ferroelect., Freq. Contr.*, vol. 49, no. 5, pp. 626–634, 2002.

[5] M. Toda and J. Dahl, "PVDF corrugated transducer for ultrasonic ranging sensor," *Sens. Actuators, A: Phys.*, vol. 134, no. 2, pp. 427–435, 2007, [Online]. Available: www.scopus.com.

[6] A. Fiorillo, "Design and characterization of a PVDF ultrasonic range sensor," *IEEE Trans. Ultrason., Ferroelect., Freq. Contr.*, vol. 39, no. 6, pp. 688–692, 1992.

[7] J. L. Ealo, A. R. Jimenez, F. Seco, C. Prieto, J. Roa, F. Ramos, and J. Guevara, "Broadband omnidirectional ultrasonic transducer based on EMFi for air ultrasound," in *Proc. IEEE Ultrason. Symp.*, 2006, pp. 812–815.

[8] A. H. M. Hazas, "Broadband ultrasonic location systems for improved indoor positioning," *IEEE Trans. Mobile Comput.*, vol. 5, pp. 536–546, 2006.

[9] J. Hillenbrand and G. Sessler, "High-sensitivity piezoelectric microphones based on stacked cellular polymers films," *J. Acoust. Soc. Amer.*, vol. 116, pp. 3267–3270, 2004.

[10] J. Alametsa, E. Rauhala, E. Huupponen, A. Saestamoinen, A. Varri, A. Joutsen, J. Hasan, and S.-L. Himanen, "Automatic detection of spiking events in EMFi sheet during sleep," *Med. Eng. Phys.*, vol. 28, pp. 267–275, 2006.

[11] H. Sorvoja, V. Kokko, R. Myllyla, and J. Miettinen, "Use of EMFi as a blood pressure pulse transducer," *IEEE Trans. Instrum. Meas.*, vol. 54, pp. 2505–2510, 2005.

[12] G. Evreinov and R. Raisamo, "One-directional position-sensitive force transducer based on EMFi," *Sens. Actuators A*, vol. 123–124, pp. 204–209, 2005.

[13] A. Streicher, R. Muller, H. Peremans, and R. Lerch, "Broadband ultrasonic transducer for a artificial bat head," in *Proc. IEEE Ultrason. Symp.*, 2003, pp. 1364–1367.

[14] A. Streicher, M. Kaltenbacher, R. Lerch, and H. Peremans, "Broadband EMFi ultrasonic transducer for bat research," in *Proc. IEEE Ultrason. Symp.*, 2005, pp. 1629–1632.

[15] R. Lerch, A. Streicher, and A. Sutor, "Broadband ultrasonic transducer," in *Proc. 19th Int. Congr. Acoust. (ICA2007)*, Madrid, 2007, pp. 1–6.
[16] R. Kressmann, "New piezoelectric polymer for air-borne and waterborne sound transducers," *J. Acoust. Soc. Amer.*, vol. 109, no. 4, pp. 1412–1416, 2001.
[17] L. A. Whitehead and B. J. Bolleman, "Microstructured elastomeric electromechanical film transducer," *J. Acoust. Soc. Amer.*, vol. 103, no. 1, pp. 389–395, 1998.
[18] M. J. Anderson, J. A. Hill, C. M. Fortunko, N. S. Dogan, and R. D. Moore, "Broadband electrostatic transducers: Modeling and experiments," *J. Acoust. Soc. Amer.*, vol. 97, no. 1, pp. 262–272, 1995.
[19] M. Paajanen, H. Valimiiki, and J. Lekkala, "Modelling the sensor and actuator operations of the electromechanical film emfi," in *Proc. IEEE 10th Int. Symp. on Electrets*, 1999, pp. 735–738.
[20] E. Tuncer, M. Wegener, and R. Gerhard-Multhaupt, "Modeling electromechanical properties of layered electrets: Application of the finite-element method," *J. Electrostat.*, vol. 63, no. 1, pp. 21–35, 2004.
[21] P. M. Morse and K. U. Ingard, *Theoretical Acoustics*. Princeton, NJ: Princeton University Press, 1968.
[22] E. Williams, *Fourier Acoustics. Sound Radiation and Nearfield Acoustic Holography*. London: Academic Press, 1999.
[23] X. Zhang, J. Hillenbrand, and G. Sessler, "Improvement of piezoelectric activity of cellular polymers using a double-expansion process," *J. Phys. D: Appl. Phys.*, vol. 37, pp. 2146–2150, 2004.

Joao Luis Ealo has been a tenured lecturer of the School of Mechanical Engineering of the University of Valle, Cali, Colombia, since 2002. He was born in Cartagena de Indias, Colombia, in 1976. He received the B.Sc. degree in mechanical engineering from the University of Ibagué, Colombia, in 1998, and the M.Sc. degree in industrial control systems from the University of Valladolid, Spain, in 2000. Mr. Ealo is currently pursuing a doctorate degree in mechanical engineering at the Polytechnic University of Madrid, Madrid, Spain, supported by the Instituto de Automática Industrial, Consejo Superior de Investigaciones Cientificas (CSIC), and the University of Valle. Currently he is working under the supervision of Fernando Seco in the modelling and design of air-borne ultrasonic transducers based on piezoelectret film.

Fernando Seco was born in Madrid, Spain, in 1972. He obtained a degree in physics from the Universidad Complutense of Madrid in 1996 and a Ph.D. degree in physics from the Universidad Nacional de Educación a Distancia (UNED), Madrid, in 2002; his dissertation dealt with the generation of ultrasonic waves applied to a magnetostrictive linear position sensor. Since 1997 he has been working at the Instituto de Automática Industrial-CSIC in Arganda del Rey, Madrid, where he holds a research position. His main research interest lies in the design and development of local positioning systems (LPS), especially those based on ultrasound and radio frequency identification (RFID), and specifically on the topics of modulation and codification of ultrasonic signals, multilateration algorithms, and Bayesian localization methods.

Antonio Ramón Jiménez graduated in physics, computer science branch (Universidad Complutense de Madrid, June 1991). He received the Ph.D. degree also in physics from the Universidad Complutense de Madrid in October 1998. From 1991 to 1993, he worked in industrial laser applications at CETEMA (Technological Center of Madrid), Spain. Since 1994, he is working as a researcher at the Instituto de Automática Industrial, CSIC, Spain. His current research interests include sensor systems (ultrasound in air, laser range-finding) and signal processing techniques for localization, feature extraction, and tracking in sectors such as robotics, vehicle navigation, inspection, personal assistance, and machine-tool.